

# The occurrence of austenitic layers in laser surface-melted iron alloys

G. PALOMBARINI, G. SAMBOGNA

*Institute of Metallurgy, University of Bologna, Viale Risorgimento 4, 40136 Bologna, Italy*

M. CARBUCICCHIO

*Department of Physics, University of Parma, Italy*

In iron alloys surface melted by power laser treatments, thin, relatively soft layers mainly constituted by austenite, can form in the upper part of the solid state transformed regions. The mechanism of formation involves both carbon diffusion from the melt, in amounts sufficient to stabilize austenite, and the high thermal gradients typically produced in the alloys by high-energy sources.

## 1. Introduction

In the field of surface treatment of metals by continuous wave power lasers, increasing interest is being directed toward processes involving rapid surface melting and cooling. This is a simple and reliable way to obtain alloying and, in general, structural modifications which could hardly be produced using conventional techniques.

In the technologically important sector of iron alloys, laser surface melting may lead to the formation of thin layers mainly constituted by austenite in the upper part of the solid state transformed regions. Generally, this austenite is large-grained, with intergranular cementite and irregularly distributed martensite (Fig. 1). The presence of these relatively soft (hardness  $\approx 4 \text{ kN mm}^{-2}$ ) "white layers" may significantly influence the mechanical properties of the treated materials. In iron alloys of different composition, white layers were observed to form depending on laser processing conditions [1–7].

The aim of the present work was to define the mechanism of white layer formation, pointing out the role exerted by: (i) laser processing conditions, and (ii) composition of base alloys and of anti-reflection coatings. The volume of the melted regions and the extent of melt–environment interactions were also considered.

## 2. Experimental procedure

Plates 10 mm thick of the steels AISI 1040, 9840 and 52100, whose composition is reported in Table I, were graphite or phosphate-coated and submitted to single-pass laser treatments in an air or helium stream. Graphite coatings were applied by spraying a suspension diluted with a binder. Phosphating was carried out by immersion in zinc phosphate solutions at 90 °C. The laser processing conditions ranged from 1.5–11.6  $\text{kW cm}^{-2}$  incident power density and 0.13–3 s interaction time.

The phase composition was determined by X-ray diffraction, using the  $\text{CoK}_\alpha$  radiation, and by surface Mössbauer measurements, by detecting the 6.4 keV X-rays and the K shell conversion electrons re-emitted by  $^{57}\text{Fe}$  atoms. Cross-sections of the treated samples were prepared for metallographic observations and microhardness measurements.

## 3. Results and discussion

Under the adopted conditions of laser treatment, the occurrence of surface melting phenomena was found to differ along with the alloy compositions and, for the same alloy, with the anti-reflection material (Tables II, III). The differences in the melting behaviour of the two steels for the same processing conditions were concerned with both the onset of melting and the melting depth.

In the absence of melting, the solid state transformations led to coarse martensite with different amounts of retained austenite, whose concentration gradually decreased on going from the surface towards the bulk. Among the treatment conditions leading to surface melting, some white layers were allowed to form in the upper part of the solid state transformed regions. In the case of the AISI 52100 steel, white layers were observed on graphite-coated samples which were treated in air at high power density and low beam–sample interaction time. In no case were white layers such as that shown in Fig. 1 formed when treating the same steel under the same processing conditions, but using phosphate compounds as anti-reflection coating.

In the case of graphite-coated samples of the medium carbon AISI 1040 and 9840 steels, white layers formed for all the treatments, giving rise to surface melting, irrespective of the processing atmosphere (air or helium stream).

Fig. 2 shows the values of melting depth as a function of incident energy, measured for the 52100

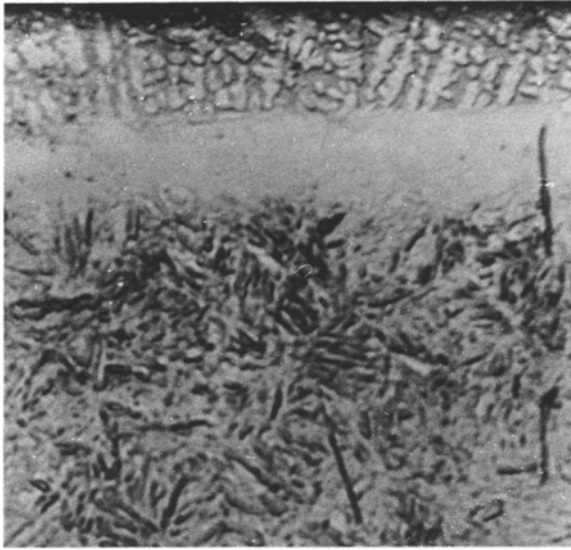


Figure 1 Metallographic cross-section of a laser surface melted AISI 9840 steel sample, showing a "white-layer" in the upper part of the solid state transformed region.

TABLE I Compositions of steels

Steel (AISI)	Element (wt%)							
	C	Si	Mn	P	S	Cr	Mo	Ni
1040	0.42	0.30	0.83	0.013	0.023	0.10	0.02	0.09
9840	0.38	0.33	0.62	0.002	0.024	0.84	0.15	0.79
52100	1.00	0.28	0.38	0.009	0.014	1.48	-	-

TABLE II Melting behaviour and WL-formation for AISI 52100 steel

Specific power (kW cm <sup>-2</sup> )	Velocity (m min <sup>-1</sup> )	Coating	Atmo-sphere	Melting	WL-formation
2	4.5	G	Air	N	N
2	4.5	P	Air	N	N
2	1.66	G	Air	N	N
2	1.66	P	Air	N	N
2	0.78	G	Air	N	N
2	0.78	P	Air	N	N
5.4	4.5	G	Air	Y	Y
5.4	4.5	P	Air	Y	N
5.4	1.66	G	Air	Y	Y
5.4	1.66	P	Air	Y	N
5.4	0.78	G	Air	Y	N
5.4	0.78	P	Air	Y	N
11.6	4.5	G	Air	Y	Y
11.6	4.5	P	Air	Y	N
11.6	1.66	G	Air	Y	N
11.6	1.66	P	Air	Y	N
11.6	0.78	G	Air	Y	N
11.6	0.78	P	Air	Y	N

WL = white layer, G = graphite, P = phosphating, N = no, Y = yes.

and 9840 steels treated in air. The different values of incident energy for the onset of surface melting for the two steels should be noted. Fig. 3 shows the average thickness of the corresponding white layers. This figure shows that:

1. No white layer forms in absence of surface melting;

TABLE III Melting behaviour and WL-formation for AISI 9840 steel

Specific power (kW cm <sup>-2</sup> )	Velocity (m min <sup>-1</sup> )	Coating	Atmo-sphere	Melting	WL-formation
2	4.5	G	Air	N	N
2	1.66	G	Air	N	N
2	0.78	G	Air	N	N
5.4	4.5	G	Air	N	N
5.4	1.66	G	Air	Y	Y
5.4	0.78	G	Air	Y	Y
11.6	4.5	G	Air	Y	Y
11.6	1.66	G	Air	Y	Y
11.6	0.78	G	Air	Y	Y

WL = white layer, G = graphite, N = no, Y = yes.

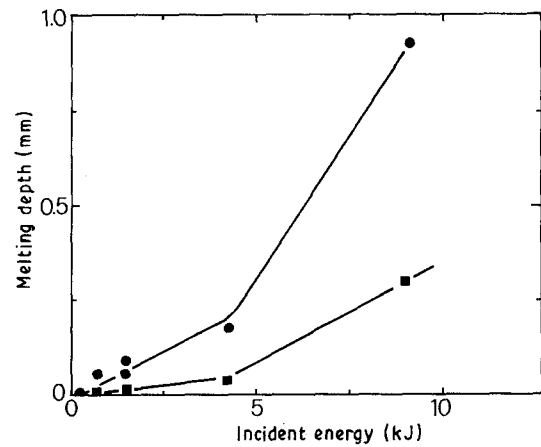


Figure 2 Values of melting depth as a function of the incident energy for AISI (●) 52100 and (■) 9840 steels laser treated in air.

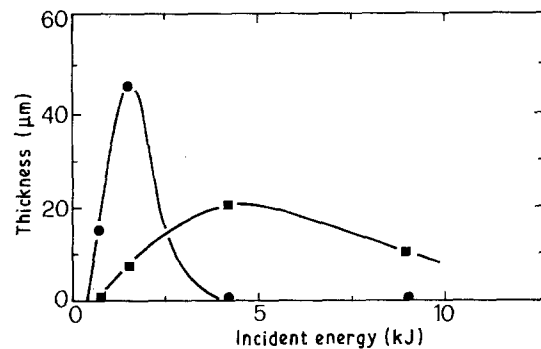


Figure 3 Average thicknesses of "white layers" formed in AISI (●) 52100 and (■) 9840 steels laser treated in air with different incident energies.

2. thicknesses increase up to maxima of about 45 μm for the 52100 steel, and about 20 μm for the medium carbon steels;

3. the energy value at the maximum is remarkably lower for the 52100 steel than for the medium carbon steels;

4. after the maxima, the white layer thickness decreases to zero very rapidly in the case of the 52100 steel, and much more slowly in the case of the medium carbon steels.

The above results can be explained on the basis of (i) carbon content in the melt, and (ii) carbon content and thermal gradient in the underlying solid region.

A higher carbon content in the base alloy (e.g. 1% C compared to 0.4% C) favours surface melting (Fig. 2). The melt can undergo a carbon enrichment from anti-reflection coatings (e.g. graphite), while carbon losses can ensue from oxidizing melt–environment interactions [6]. On the other hand, during the heating stage of the treatment, the solid region underlying the melt is austenitized to a depth which, for a given metallurgical structure, depends on the thermal gradients (temperature–depth and temperature–time). In the case of C-enriched melts, carbon easily diffuses in the underlying solid region, where conditions are established which favour the stabilization of austenite during the subsequent cooling stage.

In this region, the formation and thickness of austenitic white layers depend on the thermal gradients locally induced during the melting and cooling stages. With low temperature gradients, carbon diffuses in depth giving rise to a carbon concentration profile gradually decreasing from the melt–solid interface towards the bulk. Consequently, the distribution of retained austenite also gradually decreases. On the contrary, in the case of high gradients, carbon is led to concentrate in narrow regions of solid where, consequently, a complete stabilization of austenite is allowed.

Therefore, the formation of a front separating a region almost entirely constituted by retained austenite from an underlying almost-entirely martensitic region (Fig. 1) can occur only with the high thermal gradients which are typical of surface treatments carried out using high power sources (lasers, electron beams, etc.).

This mechanism is able to explain the differences shown in Figs 2 and 3 for different graphite-coated alloys laser treated under the same processing conditions. An early surface melting (like that occurring for the 1% C steel, Fig. 2) allows a greater amount of carbon to dissolve from the coating into the melt and subsequently to diffuse into the underlying austenitized region. In this region, the carbon distribution depends on the thermal gradient which, in turn, depends on (i) the dimensions of the sample, (ii) the thermal properties of the treated materials, and (iii) the melting depth.

Fig. 4 shows two temperature profiles expected for samples of equal thickness of the same material, laser treated at different energies and, consequently, melted to different depths. For the higher melting depth, the thickness of solid metal available for thermal conduction (i.e. for cooling) is lower, while the temperature at the melt–solid interface is substantially the same. As a consequence, the thermal gradient is also lower. From the C-enriched melt, carbon can diffuse in the solid to a greater depth than in the case of lower gradients (Fig. 5), and white layers of increasing thickness are allowed to form (Fig. 3).

However, the amount of carbon made available by the anti-reflection coating and, consequently, the extent of the increase in thickness of the white layer, are limited. An intermediate value of incident energy exists over which the carbon concentration, lowered as a result of a deeper penetration of the element in the

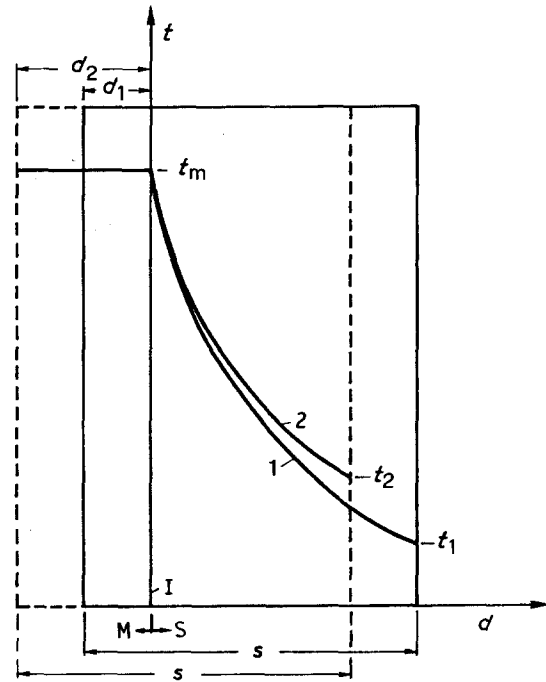


Figure 4 Thermal gradients expected in samples (—) 1 and (---) 2 of equal thickness,  $s$ , laser surface melted to different depths  $d_1$  and  $d_2$ .  $t$ , temperature;  $d$ , depth; I, melt–solid interface; M, melt; S, solid;  $t_m$ , melting temperature;  $t_1$ ,  $t_2$ , temperatures at the bottom of the samples.

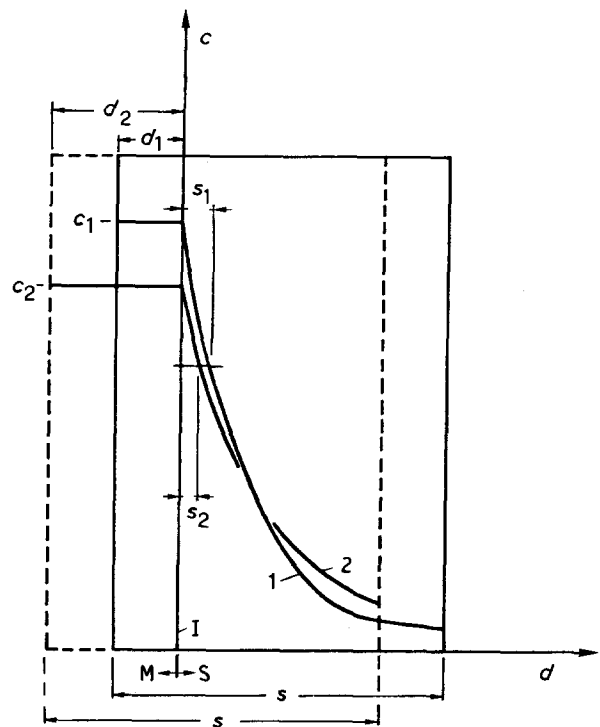


Figure 5 Carbon concentration profiles as a function of depth,  $d$ , expected for the thermal gradients shown in Fig. 4.  $c$ , carbon concentration;  $s$ , sample thickness; I, melt–solid interface; M, melt; S, solid;  $d_1$ ,  $d_2$  melting depths;  $s_1$ ,  $s_2$  “white layer” thicknesses;  $c_1$ ,  $c_2$  carbon concentration in the melts.

austenitized region, is no longer sufficient to stabilize austenite. As a consequence, white layers of decreasing thickness form during the subsequent cooling stage (Fig. 3), until conditions no longer allowing white layer formation are established.

#### 4. Conclusions

In iron alloys surface melted by laser treatments, thin layers mainly constituted by austenite can form in the upper part of the solid state transformed regions. For these white, soft layers to form, conditions are needed involving diffusion of carbon from the melt into a solid region undergoing a sufficiently high thermal gradient. In particular:

1. Austenite, formed during the heating stage of the laser treatment, may be stabilized by the diffused carbon;

2. with low gradients of temperature, carbon diffuses in depth giving rise to a gradually decreasing profile of retained austenite. With high temperature gradients, carbon is led to concentrate in narrow regions of solid giving rise to a front sharply separating an upper region of retained austenite from the underlying region having undergone the austenite-martensite transformation;

3. The thickness of white layers increases with the incident energy up to a maximum, over which the thickness decreases to zero;

4. the formation of white layers can be avoided by properly selecting the composition of base alloys to surface melt, the anti-reflection coating, and the laser processing conditions.

#### Acknowledgements

The authors thank the RTM Institute, Vico Canavese (Turin), Italy, for making available materials and laser treatments. This work was carried out with financial support from MPI, Rome, Italy, and CNR-GNSM, Rome, Italy.

#### References

1. M. CARBUCICCHIO, G. MEAZZA, G. PALOMBARINI and G. SAMBOGNA, *J. Mater. Sci.* **18** (1983) 1543.
2. M. CARBUCICCHIO and G. PALOMBARINI, *Thin Solid Films* **126** (1985) 293.
3. M. CARBUCICCHIO, G. SAMBOGNA and G. PALOMBARINI, *Hyperfine Interact.* **28** (1986) 1021.
4. M. CARBUCICCHIO and G. PALOMBARINI, *J. Mater. Sci.* **21** (1986) 75.
5. M. CARBUCICCHIO, G. LENZI, G. PALOMBARINI and G. SAMBOGNA, in "Gas Flow and Chemical Lasers", edited by S. Rosenwaks (Springer-Verlag, Berlin, 1987) p. 436.
6. M. CARBUCICCHIO, A. CASAGRANDE, G. PALOMBARINI and G. SAMBOGNA, Proceedings of the International Conference on Laser Materials Processing (LAMP'87), Osaka, Japan (High Temperature Society of Japan Ed., 1987) p. 431.
7. A. WALKER, D. R. F. WEST and W. M. STEEN, *Mater. Sci. Technol.* **11** (1984) 399.

*Received 18 June*

*and accepted 26 June 1990*